

RAPID THERMAL PROCESSING FOR FRONT AND REAR CONTACT PASSIVATION

S. Bowden, D. S Kim, C. Honsberg and A. Rohatgi
University Center for Excellence in Photovoltaic Research and Education
Georgia Institute of Technology, Atlanta, GA, 30332-0250 USA
bowden@ece.gatech.edu

ABSTRACT

Rapid firing processes are well known to allow improvements in solar cell contacts, particularly for the rear contact. Previous results characterizing the quality of a rear aluminum-alloyed back surface field have measured the effective surface recombination velocity, which depends not only on the material parameters of the back surface field, but also on the base doping. This paper shows that the determination of the recombination current density in the back surface field via photoconductance measurements is an accurate technique to measure the back surface field, independent of the base resistivity. Results show that fast firing conditions give the lowest recombination, but that the firing conditions can be altered substantially while still allowing high open circuit voltages.

INTRODUCTION

The advantages of rapid thermal processing (RTP), including low thermal budgets, fast processing times and hence low cost, are well documented [1]. In addition to these practical advantages, rapid thermal processing can also offer efficiency advantages. One area where RTP can be valuable is in contact formation. For front contacts, fast firing techniques are beneficial since a short, fast firing sequence gives a low resistance ohmic contact [2]. While an ohmic front contact is essential, fast firing conditions can have even greater benefit to the rear Al-alloyed contact. An Al-alloy rear contact can improve device performance through the formation of a back surface field (BSF) in a short time, making a high quality BSF commercially feasible. The reason that fast firing gives good results is that the fast ramp times minimizes "spiking" of the Al and makes a more uniform BSF [1].

While previous results have shown good surface passivation, the wafers used in most of these experiments have resistivities between 2 to 5 Ωcm , which introduces two complications. Firstly, the effective surface passivation of the BSF, S_{eff} , depends not only on the parameters of the BSF (lifetime, diffusivity, etc), but also on the doping in the base. Therefore, the measurements on different resistivity wafers need to be corrected to account for the lower base resistivity commonly used for commercial solar cells. With lower resistivity material, S_{eff} will be higher. Secondly, previous measurements use wafers in which the lifetime in the base may introduce some recombination, making it more difficult to extract S_{eff} .

These complications can be circumvented by using photoconductance measurements to determine the recombination saturation current in the BSF, denoted by J_{0r} . Since J_{0r} depends only on the BSF parameters, it can be directly compared to results from different experiments. In addition, J_{0r} can be measured on a high resistivity wafer, where the influence of the base recombination is negligible.

BSF RECOMBINATION MEASUREMENTS

The recombination in the rear BSF of a solar cell can be measured by multiple techniques. One method is to extract S_{eff} from quantum efficiency data. This is typically done in two ways. One is by fitting parameters with PC1D and the second is by analysis of the spectral response using methods such as that suggested by Basore [3]. Another way to characterize the BSF is to use photoconductance (PC) techniques, based either on photoconductance decay (PCD) or on quasi-steady-state photoconductance (QSS-PC) measurements. The PC can be probed either by microwave techniques or by inductive coupling. A final variant in the PC techniques is the way in which data is analyzed and the measurement conditions. Under low injection conditions, S_{eff} can be calculated directly from the absolute value of the effective lifetime. Under high injection, the value of J_0 at a diffused surface can be extracted from τ_{eff} as a function of minority carrier density. Previous studies of the BSF have focused on the extraction of S_{eff} from a rear Al-alloyed region, while here we present the analysis based on J_{0r} .

All the measurements in the paper are made using a PC tester from Sinton Consulting [4]. The measurement follows the method of Kane [5] where one side of the cell is "perfectly" passivated and the J_0 of a diffused region on the other side of the wafer is determined from the inverse lifetime as a function of carrier density. In addition to this transient method, the wafers are also measured using the QSS-PC method [6]. A full description of these two techniques is given in the manufacturer's literature and references therein [4]. Since the minority carrier lifetimes are in a range where the analysis is neither fully QSS nor transient, the generalized analysis that applies to both cases is used to calculate J_{0r} .

DESCRIPTION OF A BACK SURFACE FIELD

A back surface field (BSF) consists of a heavily doped region at the rear surface of the solar cell. The BSF can be described by an effective surface recombination velocity, S_{eff} , defined as the effective surface recombination velocity at the base-BSF interface. S_{eff} can be used to

determine the effect of the BSF on the dark current and the open circuit voltage of the solar cell.

The equation for the S_{eff} at the interface between the base and the BSF is given by [7]:

$$S_{eff} = \frac{N_{Base} D_{BSF}}{N_{BSF} L_{BSF}} e^{\frac{\Delta E_G}{kT}} \left(\frac{\frac{S_0 L_{BSF} + \tanh\left(\frac{W_{BSF}}{L_{BSF}}\right)}{D_{BSF}}}{1 + \frac{S_0 L_{BSF} \tanh\left(\frac{W_{BSF}}{L_{BSF}}\right)}{D_{BSF}}} \right) \quad (1)$$

where the L_{BSF} , D_{BSF} and W_{BSF} are respectively the lifetime, diffusivity and width of the BSF region, S_0 is the surface recombination velocity at the BSF-metal interface, N_{base} and N_{BSF} are the base and BSF doping, and ΔE_G is the band gap narrowing. This equation highlights that S_{eff} is dependant on the doping in the base, and hence the base resistivity must be accurately specified when S_{eff} values are measured and reported. For example, wafers may be specified by the manufacturer with a resistivity range of 2-5 Ωcm , but this can introduce a factor of 3 difference in S_{eff} .

An alternate way to characterize the recombination in the BSF is to measure the recombination current at the edge of the base-BSF depletion region. This current is denoted by J_R or can also be characterized by its saturation current J_{0r} . At a given voltage across the BSF, J_{0r} will depend only on the parameters of the BSF. J_{0r} can be readily and accurately measured by PC measurements using a high resistivity test wafer. The measured J_{0r} can then be converted to a S_{eff} for any base resistivity and then to an effective base saturation current, J_{0b} . Finally, J_{0b} can then be used to calculate the open circuit voltage limit according to

$$V_{oc} = \frac{kT}{q} \ln\left(\frac{J_{sc}}{J_{0b}}\right) \quad (2)$$

To calculate a relationship between J_{0r} and J_{0b} or S_{eff} , the position dependant diffusion current in the base must be determined. The diffusion current in the base of the device is given by the general equation:

$$J_B = J_{0b} \left(e^{qV/kT} - 1 \right) \quad (3)$$

where J_{0b} is the saturation current in the base, V is the applied voltage, and J_B is the diffusion current at the edge of the depletion region. A convenient form of the position dependent diffusion current is found by replacing the applied voltage, V , by the difference in the quasi-Fermi levels at the junction. By allowing the quasi-Fermi levels to vary as a function of position, the current density as a function of position can be found. The diffusion current then becomes:

$$J(x) = J_0 \left(e^{\frac{E_{Fn} - E_{Fp}}{kT}} - 1 \right) = J_0 \left(\frac{np}{n_i^2} - 1 \right) \quad (4)$$

where n and p are the position dependent carrier concentrations, and J_0 is the saturation current at a particular distance x from the junction. For p-type material, Eqn. 4 becomes:

$$J(x) = J_0 \left(\frac{np - n_i^2}{n_i^2} \right) \approx J_0 \frac{np}{n_i^2} \approx J_0 \left(\frac{n(n + N_A)}{n_i^2} \right) \quad (5)$$

At the edge of the BSF where $x = W_B$, the diffusion current equals the recombination current in the BSF. The current at this point, called J_R , can be determined from Eqn 5 as:

$$J_R(x = W_B) = J_{0r} \left(\frac{n(n + N_A)}{n_i^2} \right) \approx J_{0r} \frac{nN_A}{n_i^2} \quad (6)$$

The current at the BSF edge is also given by the boundary condition at the base-BSF interface as:

$$J_R = qn \Big|_{x=W_B} S_{eff} \quad (7)$$

Equating Eqns 6 and 7, simplifying and using a general base doping gives:

$$J_{0r} \frac{N_B}{qn_i^2} = S_{eff} \quad (8)$$

where J_{0r} is recombination saturation current density for the BSF, N_B is the base doping, q is the electronic charge and n_i is the intrinsic carrier concentration. J_{0r} can be readily measured by PCD [5] or QSS-PC [6] techniques.

Once J_{0r} is measured, it can be used to calculate the effect on a solar cell with arbitrary base doping by calculating S_{eff} from J_{0r} according to Eqn. 8, and then finding J_{0b} by:

$$J_{0b} = \frac{qDn_i^2}{N_B L_{eff}} \quad (9)$$

where the effective minority carrier diffusion length, L_{eff} , is :

$$L_{eff} = L_B \frac{1 + \frac{S_{eff} L_B \tanh\left(\frac{W_B}{L_B}\right)}{D_B}}{\frac{S_{eff} L_B \tanh\left(\frac{W_B}{L_B}\right)}{D_B} + 1} \quad (10)$$

Alternately, the J_{0b} in the solar cell can be directly calculated in terms of J_{0r} according to the equation:

$$J_{0b} = J_{0bL} \frac{J_{0r} + J_{0bL} \tanh\left(\frac{W_B}{L_B}\right)}{J_{0bL} + J_{0r} \tanh\left(\frac{W_B}{L_B}\right)} \quad (11)$$

where J_{0bL} is the ideal or wide base saturation current, calculated from Eqn. 9 using the minority carrier diffusion length L_B in place of the effective diffusion length L_{eff} .

The above procedure can be applied to any solar cell with a BSF provided that the depletion region recombination at the base-BSF junction is negligible. However, in order to measure the devices using PC techniques, the carrier concentrations are assumed to be constant across the base. Under these conditions, J_{or} is identical to J_{ob} , and can be directly used as an estimate of the V_{oc} limit. This condition is accurate for $W_B < L_B$, and J_{or} will provide an upper limit on the BSF recombination. However, for very high base resistivities, the low doping increases the J_{ob} above that of J_{or} , and hence $J_{or} = J_{ob}$ no longer holds. Overall, for moderate resistivity wafers with a high lifetime, a V_{oc} limit imposed by the rear BSF can be calculated from J_{or} without requiring the details of the diffusion length or doping in the base.

MEASUREMENT OF J_{or}

The test structures for measuring J_{or} use high resistivity (>500 Ωcm) FZ n-type substrates so that the base is in high injection during photoconductance measurements. For the measurement of J_{or} , a symmetrical structure with an Al-alloyed region on both sides is ideal, as this allows straightforward analysis of the photoconductance results. However, a symmetrical structure is difficult to achieve for an Al-alloyed BSF processed using belt furnaces, since the addition of an Al layer on the front changes the BSF properties. Printing a thick Al paste on both sides of the wafer alters the firing conditions due to thermal lag and optical effects. Hence a different BSF results if the wafer has Al-region on both sides. This is easily seen by a marked change in the appearance of the fired Al layer.

Instead of a symmetrical Al-alloyed structure, the front surface is passivated with a SiO_2 in order to achieve low front surface recombination. A thin ~10 nm oxide is grown on all substrates in a dry oxidation tube process to passivate both sides of the wafer. Al is screen printed onto one side of the wafer fired at varying temperatures and times. The firing process is in air and degrades the quality of the passivating oxide. Consequently, the wafer is annealed in 4% hydrogen (forming gas anneal, FGA), at 400 °C for 15 to 30 min to recover oxide quality after the Al-alloy step. The time of the FGA anneal had no impact on the results, and the low FGA temperature has little effect on the Al BSF.

To monitor the substrate minority carrier lifetime and the effectiveness of the oxide surface passivation, a control wafer without the printed Al is processed with the other test structures. The effective lifetime of the control sample is 1.8 msec, indicating that the impact of either the front surface or the bulk is low, as expected from high resistivity wafers.

Apart from the control wafers, the test structures have a thick layer of highly conductive Al on the rear that introduces an additional conductive layer and alters the photoconductivity measurement. Consequently, the Al-alloyed layer was removed in a standard RCA2 clean. This typically leaves a residue of aluminum oxide and other paste binders. These binders can be wiped off, but

as they are not conductive, they do not alter the conductivity measurements. The removal of the Al layer may improve the surface recombination velocity at the rear of the device, but since the BFS used in these wafers are thick, S_{eff} does not depend on the surface recombination velocity at BSF-metal interface.

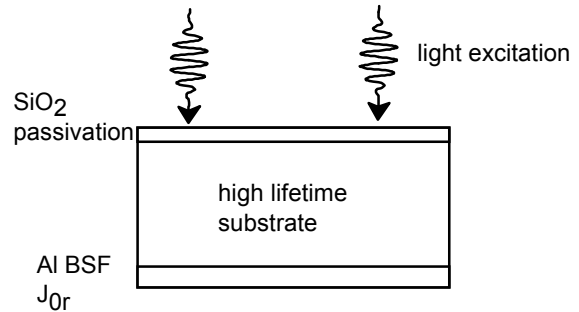


Figure 1: Test structure used to measure J_{or} , the recombination current in the rear BSF. For J_{or} measurements the substrate is high resistivity.

The measurements of J_{or} on the test structure and the firing conditions are shown in Table 1. The condition for the temperature varying profile is 435 °C, 585 °C, and 752 °C for the three furnace zones. Table 1 indicates that the optimum processing condition occurs at faster belt speeds and rapid changes in temperature. Since the front and rear surfaces are not identically passivated, the photoconductance measurements are made with the oxide-passivated side facing the light source and also with the oxide-passivated side on the stage. Infra-red light is also used ensure that the carriers are uniformly generated across the base. As Table 1 shows, the measurements from both sides are essentially identical, indicating that the difference in surface passivation does not affect the measurements. In all following analyses, the average of the two J_{or} measurements is used.

Table 1: Measurement of J_{or} from high resistivity (>500 Ωcm) FZ test structures.

Wafer	Belt Speed in/min	Temp °C	J_{or} A/cm ² front	J_{or} A/cm ² rear
N1	80	800	7.5×10^{-13}	9.2×10^{-13}
N2	15	800	1.1×10^{-12}	1.5×10^{-12}
N3	80	Varies	4.2×10^{-12}	4.1×10^{-12}

J_{or} can be used to calculate S_{eff} and the V_{oc} limits for the base resistivities used in other measurements or in commercial solar cells. Table 2 shows the results calculated from Eqns, 8, 10, 9 and 2 for 1 and 5 Ωcm material, assuming a value of 400 μsec for the base lifetime. In all subsequent calculations, the lifetime of the base is left constant at 400 μsec since the actual doping dependence will depend on the specifics of the material defects and processing conditions of the base material. The values of V_{oc} and S_{eff} are calculated at 25 °C, the

temperature at which the devices are measured, and hence n_i is $8.6 \times 10^9 \text{ cm}^{-3}$. The V_{oc} limits are calculated assuming a J_{sc} of 33 mA/cm^2 . The results in Table 2 show that for $1 \text{ } \Omega\text{cm}$ material, the V_{oc} limit is not a strong function of J_{or} despite substantial differences in S_{eff} values. In many commercial devices, the emitter contribution to the saturation current would limit the device to lower open circuit voltages. This result is important, since it indicates flexibility in implementing a high quality BSF, and hence increases the possibility that the BSF formation can be combined with other high temperature processing steps. As expected, higher resistivity materials are more sensitive to the quality of the BSF, and for such substrates an optimum BSF is required.

Table 2: Calculated V_{oc} limits and S_{eff} values for the different processing conditions on 1 and 5 Ωcm material.

#	J_{or} A/cm^2	V_{oc} limit mV 1 Ωcm	S_{eff} cm/sec 1 Ωcm	V_{oc} limit mV 5 Ωcm	S_{eff} cm/sec 5 Ωcm
N1	8.35×10^{-13}	649	1065	631	145
N2	1.3×10^{-12}	645	1660	625	225
N3	4.15×10^{-12}	638	5300	608	720

Table 2 allows comparison between the S_{eff} results calculated here and the measured S_{eff} values from other authors. For example, Lölgen reported results of 200 cm/sec on 2-5 Ωcm material [8]; Narasimha extracted $S_{eff} = 200 \text{ cm/sec}$ on 2.3 Ωcm material from spectral response measurements [1], and Lempinen reported 600 cm/sec using 2-3 Ωcm material [9] when combining the Al-alloy step with other parts of the process.

The measured J_{or} can be used to calculate the effect of the back surface field on a variety of different substrate resistivities. Figure 2 plots the V_{oc} limit from the base as a function of base resistivity. Figure 2 shows that even with a constant J_{or} , the S_{eff} changes by more than an order of magnitude. Despite the high S_{eff} at low base resistivities, the V_{oc} limit is high, due to the fact the rear surface has little impact. The actual V_{oc} would be lower than these values due to the assumption of 400 μsec in the calculations. At moderate base resistivities, the device is dominated by the rear surface, and $J_{or} \approx J_{ob}$. At higher base resistivities than shown in Figure 2, low doping in the base increase J_{ob} , and hence the base again dominates the V_{oc} limit.

CONCLUSION

Rapid fired rear Al-alloy contacts allow a BSF with very low recombination. However, the S_{eff} values commonly used to characterize the BSF depend on the base doping, and therefore are not the most appropriate way to characterize the BSF. Instead of S_{eff} , J_{or} can be used, which is independent of base doping. J_{or} can then be used to either calculate J_{ob} or S_{eff} . Measurements of J_{or} under different conditions show that fast belt speeds give the lowest recombination BSFs, but that even under less

optimum firing conditions, a high open circuit voltage limit from the rear surface can still be achieved on low resistivity material.

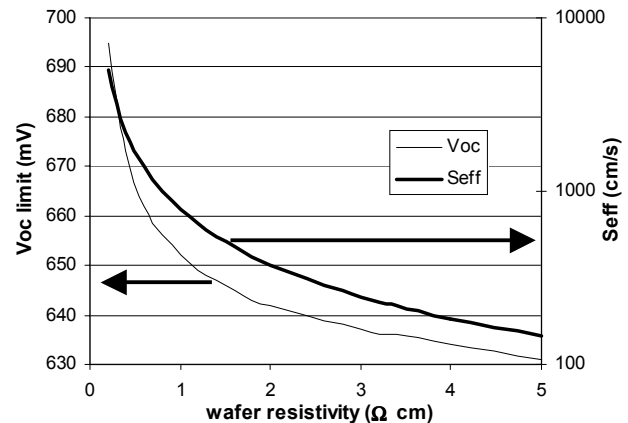


Figure 2: Calculated V_{oc} and S_{eff} as a function of base resistivity, using the optimum J_{or} from Table 2.

REFERENCES

- [1] S. Narasimha, A. Rohatgi, and A. W. Weeber, "An Optimized Rapid Aluminum Back Surface Field Technique for Silicon Solar Cells", *Transactions on Electron Devices*, 46 (7), pp. 1363-1370 (1999)
- [2] A. Laugier, H. El Omari, J.P. Boyeaux, B.Hartiti, J.C. Muller, and N. Le Quan Nam; "Rapid thermal sintering of the metallizations of silicon solar cells," *1st WPVSC*, pp.1535-8 (1994).
- [3] P.A. Basore, "Extended Spectral Analysis of Internal Quantum Efficiency", *23rd IEEE PVSC*, pp. 147 (1993)
- [4] R. A. Sinton "User Manual WCT-100 Photoconductance Tool" (2001)
- [5] D. E. Kane, and R. M. Swanson, "Measurement of the Emitter Saturation Current by a Contactless Photoconductivity Decay Method", *18th IEEE PVSC*, p. 578, (1985).
- [6] A. Cuevas, "The effect of emitter recombination on the effective lifetime of silicon wafers", *Solar Energy Materials and Solar Cells*, vol.57. no.3, p.277-90, (1999).
- [7] A. Rohatgi, "Design, Fabrication and Analysis of 17-18 Percent Efficient Surface Passivated Silicon Solar Cells", *Transaction on Electron Devices*, 31 (8), p. 596 (1984)
- [8] P. Lölgen, C. Leguijt, J.A. Eikelboom, R.A., Steeman, W.C. Sinke, L.A.Verhoef, P.F.A., Alkemade and, E. Algra, "Aluminum Back Surface Field Doping Profiles With Surface Recombination Velocities Below 200 cm/s", *23rd IEEE PVSC*, p. 236 (1993).
- [9] V-P. Lempinen, J. Harkonen and J. Kylmaluoma, M. Rajatora, and T. Marjamaki, "Single Furnace-Step Processed Large Area MC-Si Solar Cells", *28th IEEE PVSC*, pp. 241-243 (2000)